SCIENCE CHINA
Technological Sciences

Special Topic: Current Progress in Solid Mechanics and Physical Mechanics
•Article•

May 2019 Vol.62 No.5: 721–728
https://doi.org/10.1007/s11431-018-9424-4

A study of indentation scaling relationships of elastic-perfectly plastic solids with an inclusion near the conical indenter tip

YU ZhiJie & WEI YueGuang*

Department of Mechanics and Engineering Science, College of Engineering, Peking University, Beijing 100871, China

Received October 8, 2018; accepted December 26, 2018; published online March 29, 2019

Indentation hardness is found to be related to indentation depth when indentation test is applied on homogeneous materials under small indentation depth, which shows strong size effect in the indentation. While in contrast, indentation hardness has a very limited relationship with indentation depth when it is large, showing distinct scaling relationships between hardness and material properties. Previous studies on scaling relationships under deep indentation condition of elastic-perfectly plastic homogeneous materials have been carried out systematically by finite element analysis. In this paper, a heterogeneous material, particle-reinforced matrix composite is detailed studied to investigate its scaling relationships under deep indentation with different particle positions and material properties by finite element analysis.

conical indentation, elastic-perfect plastic, grain composite, scaling relationships

Citation: Yu Z J, Wei Y G. A study of indentation scaling relationships of elastic-perfectly plastic solids with an inclusion near the conical indenter tip. Sci China Tech Sci, 2019, 62: 721–728, https://doi.org/10.1007/s11431-018-9424-4

1 Introduction

Indentation tests have taken important positions of mechanical tests of materials for more than a hundred years. Comparing with other test methods, indentation test has an advantage of convenient procedure and fast response, especially at small length scales. The quasi-static and dynamic indentation tests are able to collect the message of load-displacement curve, indentation contact morphology and the recovery of the indentation residual, which helps to obtain the elastic modulus, indentation hardness and other mechanical properties of materials. Stilwell and Tabor [1] suggested to calculate material mechanical properties from the elastic recovery of the indentation test very early, which was soon applied experimentally [2,3]. Oliver and Pharr [4] proposed a well-known method to determined hardness and other material properties by indentation test, thus indentation test became one of the most used methods in material testing.

For metal materials, indentation tests are considered as deep ones while indentation depth is larger than submicrons, otherwise are deemed to be shallow ones. Many representative researches have been applied about deep indentation tests, one of which was to obtain material properties by fitting the loading and unloading load-displacement curve with finite element analysis [5]. The scaling relationships of elastic-perfectly plastic materials in indentation were found by comparison with Oliver-Pharr method and Johnson's spherical cavity model [5–7]. Indentation method was also widely used to find material properties of heterogeneous materials [8–10]. And for indentation with small depth, many cross-scale models are brought forward to explain the intensive size effect in micro- and nano-indentation tests. Strain gradient theory and surface energy model are two typical models depicting the cross-scale feature of mechanical properties in micro- and nano-indentation tests [11–21].

In recent years, micro- and nano-indentation tests are extensively used together with the relevant numerical simula-

*Corresponding author (email: weiyg@pku.edu.cn)

tions in characterizing materials. Sun et al. [22] calculated the fracture toughness of ceramics obtained from finite element method by virtual crack closure technology (VCCT), showing high accuracy comparing with experiments. Finite element method has relatively low cost and high stability, which makes it a useful method in indentation tests. Meanwhile, many simulation models and calculation methods were studied and developed correspondingly [23,24]. Mechanical properties of new materials [25–32] and their mechanical response under multi-physics fields [33–35] were systematically researched.

The validity of indentation tests is of much significance; many studies have been carried out on the system error and the validity of indentation tests. The convenience and preciseness of indentation tests were widely accepted under deep indentation [5–7,36]. However, there is still much that is not clear. For instance, whether the scaling relationships of homogeneous materials are sensitive to the inclusion, impurity or defect. This paper aims at the deep indentation of the particle-reinforced matrix composite to find the heterogeneity's influence on the scaling relationships of homogeneous elastic-perfectly plastic materials by dimensional analysis and finite element analysis, studying the hard particle-soft matrix composite and the spherical hole-matrix circumstances. By focusing on the particle or defect position's and size's influence on the indentation response, the scaling relationships of heterogeneous materials are studied and the relations between indentation hardness, contact area, load-displacement curve and indentation depth are also considered.

2 Dimensional analysis

For indentation experiment, the general parameters needed to be controlled are the indenter and the mechanical properties of the test base, namely, the half angle of the conical indenter (θ), Young's modulus (E), yield strength (Y) and Poisson's ratio (ν) of the elastic-perfectly plastic matrix. With the consideration of grain impurity, Young's modulus (E_g) and Poisson's ratio (ν_g) of the grain are needed. Since the particle is taken to be elastic for simplicity, the plastic parameters are not considered. Along with the mechanical properties, parameters for geometric appearance of the particle-reinforced matrix composite are also needed, namely, the diameter of the spherical particle (d) and the depth form the upper surface of the particle to the surface of the matrix (D). The distribution of the inclusions in the matrix could be unpredictable, to simplify the simulation model, the influence of all particles but the closest is neglected. The rationality of this simplification is also discussed in later calculation. The simplified model is shown in Figure 1.

The conical indenter is supposed to be rigid, the position of the indentation is right above the particle, the axis of the conical indenter is collinear with the normal of the matrix surface and particle's diameter. Friction between indenter and matrix is supposed to be zero. Though there is no analytic solution to this problem, the dimensional analysis could help to obtain some useful scaling relationships.

As in Figure 1, parameters in indentation needed to be considered are the load (F) and displacement (h) of the indenter and the morphology of the indentation area, namely, the contact depth (h_c) and the contact radius (r). With the contact depth (h_c) and the half angle of the indenter (θ), the contact radius (r) can be calculated by

$$r = h_c \tan\theta, \tag{1}$$

thus the indentation hardness (H) is defined as

$$H = \frac{F}{\pi r^2}. \tag{2}$$

In all variables and parameters mentioned above, the load of indenter (F) and the contact depth (h_c) are taken to be functions of other variables as

$$F = f_l(E, Y, \nu, E_g, \nu_g, d, D, h, \theta), \tag{3}$$

$$h_c = g_h(E, Y, \nu, E_g, \nu_g, d, D, h, \theta). \tag{4}$$

In eqs. (3) and (4), the variables are composed with only dimension of modulus and length. Taking Young's modulus of the matrix (E) and the displacement of the indenter (h) as two independent variables, other variables can be expressed as

$$\begin{aligned} &[Y] = [E]^1[h]^0,\ [E_g] = [E]^1[h]^0,\ [D] = [E]^0[h]^1,\\ &[d] = [E]^0[h]^1,\ [\theta] = [E]^0[h]^0,\ [\nu] = [E]^0[h]^0,\\ &[F] = [E]^1[h]^2,\ [h_c] = [E]^0[h]^1,\ [\nu_g] = [E]^0[h]^0. \end{aligned} \tag{5}$$

With the application of Π theory, the load of indenter (F) and the contact depth (h_c) could be written as

$$F = Eh^2 \prod_1\left(\frac{E}{Y}, \frac{E}{E_g}, \frac{h}{d}, \frac{D}{d}, \nu, \nu_g, \theta\right), \tag{6}$$

$$h_c = h \prod_2\left(\frac{E}{Y}, \frac{E}{E_g}, \frac{h}{d}, \frac{D}{d}, \nu, \nu_g, \theta\right). \tag{7}$$

Substituting eq. (2) into eqs. (6) and (7), the indentation hardness (H) could be non-dimensionalized as

$$\begin{aligned} \frac{H}{Y} &= \frac{F}{Y\cdot \pi h_c^2 \tan^2\theta}\\ &= \frac{E\cdot h^2}{Y\cdot \pi\tan^2\theta\cdot h^2}\cdot\frac{\prod_1\left(\frac{E}{Y}, \frac{E}{E_g}, \frac{h}{d}, \frac{D}{d}, \nu, \nu_g, \theta\right)}{\prod_2^2\left(\frac{E}{Y}, \frac{E}{E_g}, \frac{h}{d}, \frac{D}{d}, \nu, \nu_g, \theta\right)}\\ &= \prod_3\left(\frac{E}{Y}, \frac{E}{E_g}, \frac{h}{d}, \frac{D}{d}, \nu, \nu_g, \theta\right), \end{aligned} \tag{8}$$

where $\Pi_1 = \frac{F}{Eh^2}$, $\Pi_2 = \frac{h_c}{h}$, $\Pi_3 = \frac{H}{Y}$ and other variables in

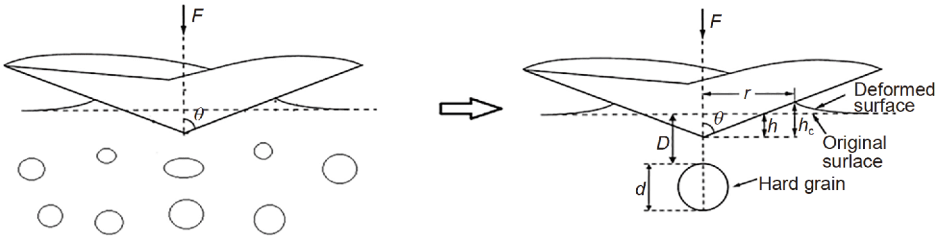

Figure 1 The particle-reinforced matrix composite and simplified axisymmetric model.

these three functions are all dimensionless. It's worth noting that for the circumstances of grain-matrix composite, there are 7 independent variables in the dimensionless functions, but for the homogeneous situation the number of independent variables shrinks to 3, which is the same with the situation of the composite with all inclusions at an infinite distance away from the surface, then eqs. (6)–(8) could then be written as follows [5–7]:

$$\begin{aligned} F &= Eh^2\prod_4\left(\frac{E}{Y},\nu,\theta\right),\\ h_c &= h\prod_5\left(\frac{E}{Y},\nu,\theta\right),\\ H &= Y\prod_6\left(\frac{E}{Y},\nu,\theta\right). \end{aligned} \tag{9}$$

In eq. (9), Π_4, Π_5 and Π_6 are irrelevant with indenter displacement h. Hence in this homogeneous situation, when $\frac{E}{Y},\nu,\theta$ are token to be constant, the load of the indenter (F) is proportional to the square of h, the contact depth (h_c) is proportional to h and the indentation hardness (H) is proportional to the yield strength of the matrix (Y). However, for the grain composite, these relations would be influenced by other parameters.

In addition, to find the relationship in the load-displacement curve and the calculation of Young's modulus from the curve, the derivative of eq. (6) is non-dimensionalized as

$$\begin{aligned} &\left(\frac{1}{Eh_m}\right)\frac{\mathrm{d}F}{\mathrm{d}h}\bigg|_{h=h_m}\\ &=\left(\frac{1}{Eh_m}\right)\left[\prod_1\cdot\frac{\mathrm{d}(Eh^2)}{\mathrm{d}h}+Eh^2\cdot\frac{\mathrm{d}}{\mathrm{d}x}\prod_1\right]\bigg|_{h=h_m}\\ &=2\prod_1\left(\frac{E}{Y},\frac{E}{E_g},\frac{h_m}{d},\frac{D}{d},\nu,\nu_g,\theta\right)\\ &\quad+\frac{h_m}{d}\prod_1'\left(\frac{E}{Y},\frac{E}{E_g},\frac{h_m}{d},\frac{D}{d},\nu,\nu_g,\theta\right)\\ &=\prod_7\left(\frac{E}{Y},\frac{E}{E_g},\frac{h_m}{d},\frac{D}{d},\nu,\nu_g,\theta\right), \end{aligned} \tag{10}$$

where h_m is an arbitrary indenter displacement. From eq. (10) the corresponding Young's modulus could be estimated from the value of the dimensionless function Π_7.

Dimensionless functions help to reveal laws between different variables and reduce parameter dependency of experiments, thus a reasonable selection of dimensionless functions could give much instruction to experiments and simulations.

3 Finite element analysis

In this paper, the commercial finite element software ABAQUS is used to simulate the indentation test, from which the scaling relationships of indentation is acquired together with the inspirations from dimensional analysis.

A conical indenter with a half angle of 68° is chosen as Bhattacharya et al. [3] did. The Poisson's ratio of 0.2 for both the particle (ν_g) and matrix (ν) is chosen and Young's modulus of hard grain (E_g) is 100 times that of the matrix (E), namely E_g=100E. Unless otherwise stated, the above relationships of parameters remain unchanged in this paper. Due to the application of dimensionless functions, some parameters could be fixed with no influence to the scaling relationships, in this paper, the diameter of spherical grain (d) and the yield strength of the matrix (Y) are fixed, thus related variables $\frac{E}{Y}$, $\frac{D}{d}$ and $\frac{h}{d}$ are all controlled by only one parameter.

The simplified model is axisymmetric about the collinear lines of the axis of the conical indenter and the spherical grain. Such that an axisymmetric simulation model is used to substitute the 3D entity to reduce the calculation cost. The length of the whole analysis area is 100 times the radius of the grain, hence this finite size model could be considered as an infinite half space. Each different geometry of the composite corresponds with one different model and a different set of mesh. For each model, the number of the mesh is in the range from 8000 to 10000, and these meshes of all models pass the mesh convergence test to minimize the divergence from different meshes. All meshes are chosen to be 4-node bilinear axisymmetric quadrilateral meshes. The general mesh distribution and the refined area near the indenter and the grain are shown in Figure 2.

The indenter load (F) and displacement (h) are extracted from the reaction force and the vertical displacement of the reference point on the indenter. The contact depth (h_c) is

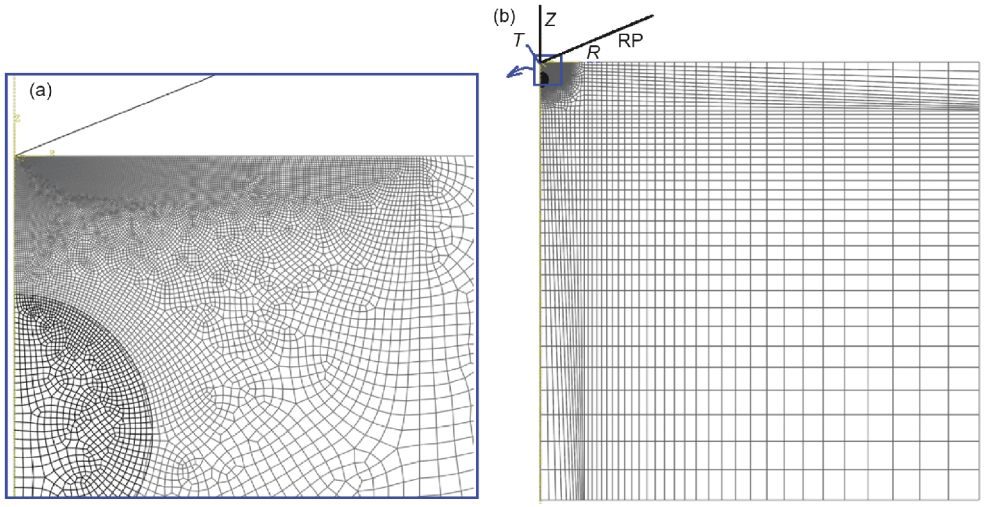

Figure 2 (Color online) Mesh of the axisymmetric model and the refined zone. (a) Refined mesh near the indenter and the inclusion; (b) global mesh.

obtained from the total contact area of ABAQUS(CAREA) and the half angle of the indenter (θ), and by eqs. (1) and (2), the indentation hardness (H) could be calculated. The simulation and result are carried out by ABAQUS CAE/Standard, version 6.14.

4 Results and discussion

Figure 3 shows the relationship of dimensionless functions $\prod_1 = \frac{F}{Eh^2}$ and $\prod_2 = \frac{h_c}{h}$ with the indenter displacement (h) in a grain composite indentation with the matrix material of $\frac{E}{Y}$=20 and are compared with Cheng et al. [5–7] result of homogeneous materials with same matrix property. Since Π_1 and Π_2 are related with the dimensionless indentation depth $\frac{h}{d}$, these two dimensionless functions are still depth related and the value of Π_1 and Π_2 ascend with the dimensionless indentation depth. This relationship will be discussed detailedly in the following part.

The influence of heterogeneity is mostly concentrated near the indenter and the impurity, so the grain depth and the indenter displacement are most relating variables of dimensionless functions Π_1, Π_2 and Π_3. Figure 4 gives the figures of Π_1, Π_2 and Π_3 against the dimensionless indentation depth with different geometric morphology, namely the dimensionless grain depth ($\frac{D}{d}$=0.02, 0.05, 0.1, 0.5, 1, 2, inf), with matrix property fixed at $\frac{E}{Y}$=20. It is clear that in the homogeneous model the dimensionless grain depth does not affect Π_1, Π_2 or Π_3. While with the dimensionless depth of hard grain descending from infinity to 0.02, values of these three dimensionless functions ascend correspondingly. The

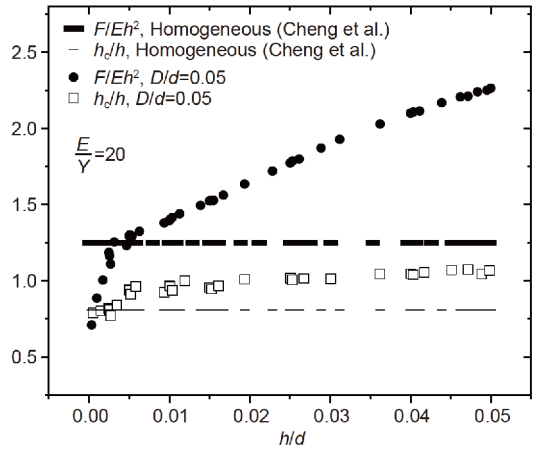

Figure 3 Influence of heterogeneous structure on dimensionless load and contact depth.

dimensionless load, Π_1, ascends most monotonically and shows very clear laws, and the changing of Π_1 is also larger than Π_2 and Π_3. In the situation of $\frac{D}{d}$=0.02 and $\frac{E}{Y}$=20, this largest change rate reaches 200%. Meanwhile, Π_3 only changes slightly around 30%. Furthermore, the dimensionless load of indenter indenting into the original position of the upper surface of the hard grain varies rapidly, showing intensive size effect.

Figure 5 shows different matrix properties' influence ($\frac{E}{Y}$=20, 50, 100, 200, 500, 1000, 2000) on dimensionless functions Π_1, Π_2 and Π_3 against dimensionless indentation depth of fixed composite geometry $\frac{D}{d}$=0.02. Hard grain increases the dimensionless indentation contact depth Π_2 and load Π_1 with the increase of dimensionless indentation depth $\frac{h}{d}$, besides, this increment is also monotonous with the

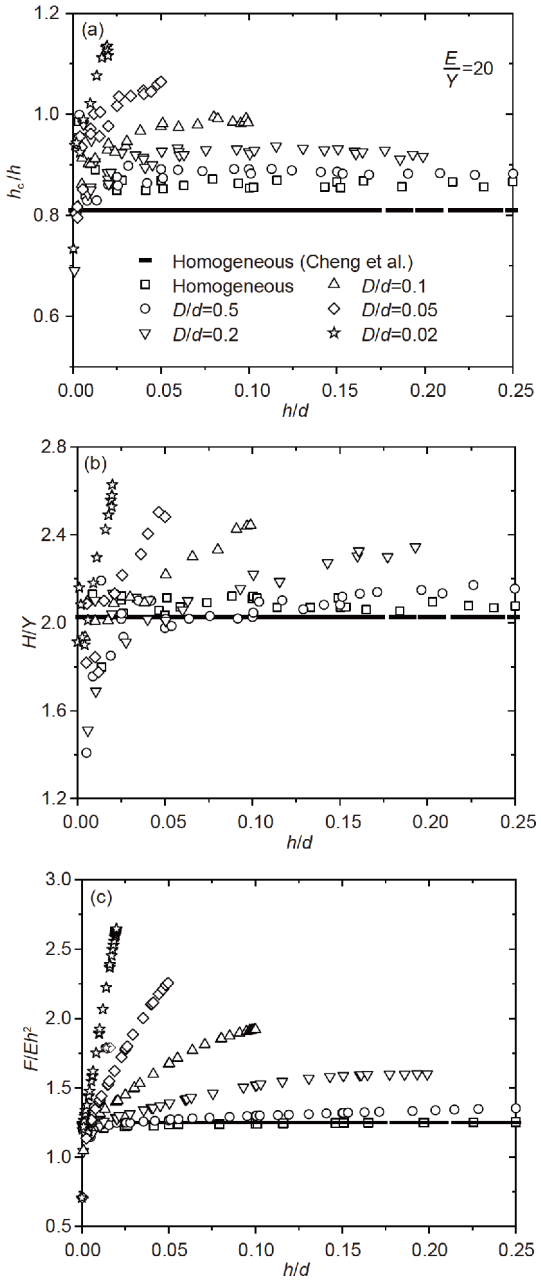

Figure 4 Dimensionless functions, Π_2 (a), Π_3 (b) and Π_1 (c), against the dimensionless indentation depth of different heterogeneities. Figures without legend share the legend of previous ones.

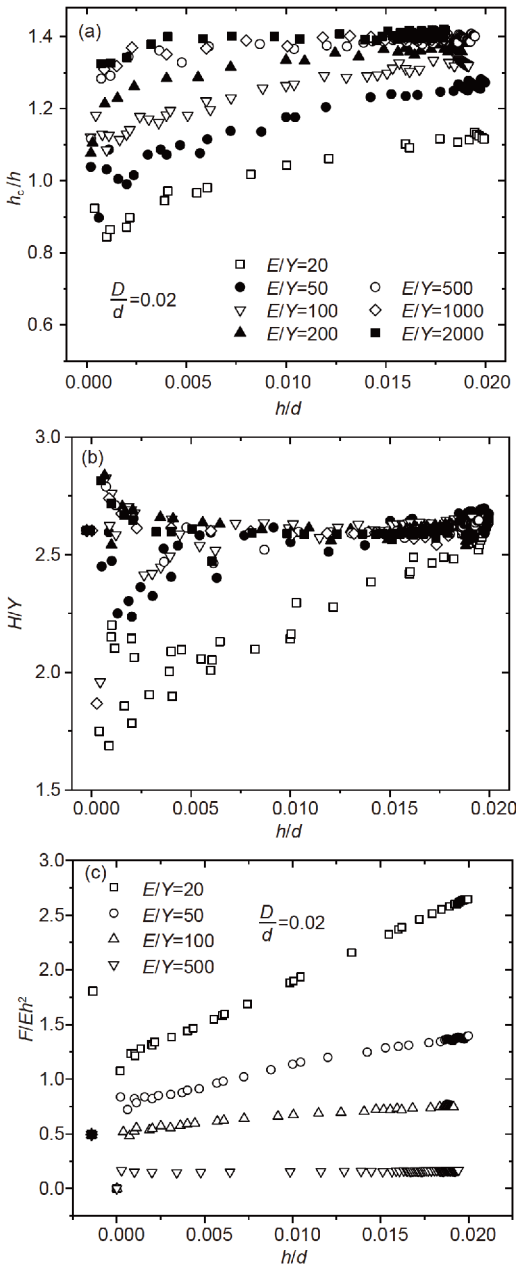

Figure 5 Dimensionless functions, Π_2 (a), Π_3 (b) and Π_1 (c), against the dimensionless indentation depth of different dimensionless matrix modulus.

change of dimensionless matrix modulus. Meanwhile, the dimensionless hardness Π_3 does not have a monotonous with either indentation depth or material modulus, for the case of $\frac{E}{Y}$=20, an apparent increase could be found with the increase of dimensionless indentation depth, for cases of other modulus, Π_3 does not change much, and for all cases of modulus, it seems that the dimensionless indentation hardness tends to a value around 2.6 with the increase of dimensionless indentation depth.

In addition to the study on hard grain's reinforcement of the matrix, the influence of soft grain on the matrix is also discussed. By processing the same procedure of a soft grain which has smaller elastic modulus than the matrix, a porous problem or the softening effect could be understood and might help to compare with the hard grain's cases. Figure 6 shows the same variables and dimensionless functions with Figure 5, the only difference is that the elastic modulus of the grain, changes from 100 times that of the matrix to one-tenth of the modulus of the matrix. After altering the hard-soft relation of grain-matrix, the dimensionless load Π_1 and contact depth Π_2 show nearly completely opposite relation-

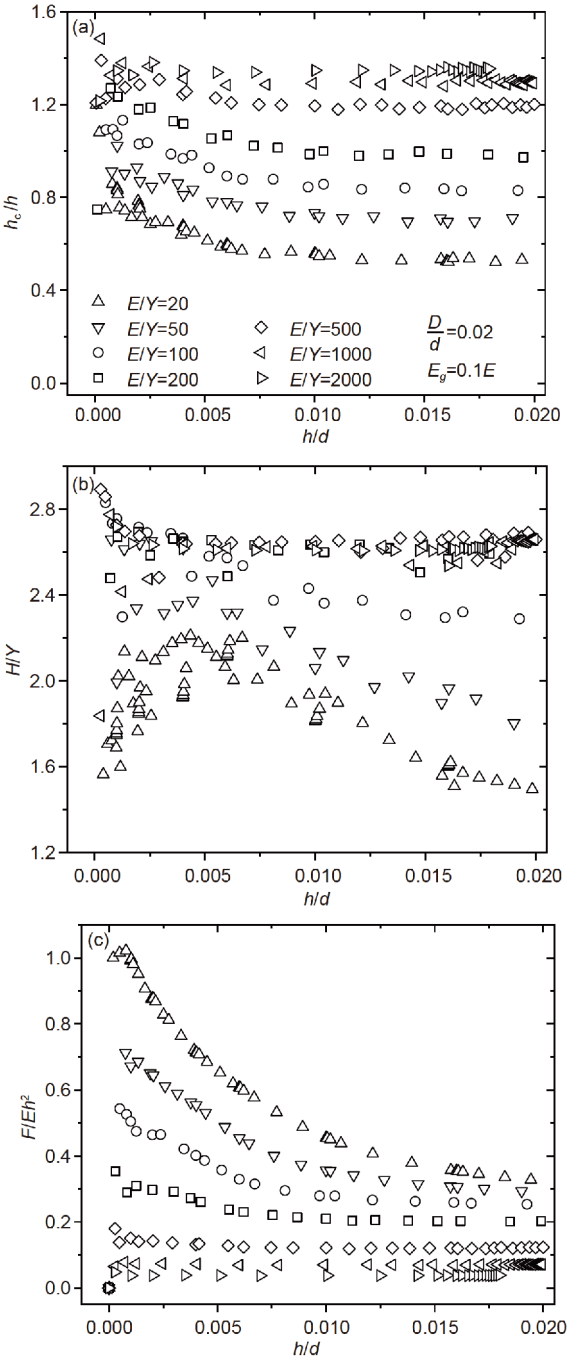

Figure 6 Dimensionless functions, Π_2 (a), Π_3 (b) and Π_1 (c), against the dimensionless indentation depth of different dimensionless matrix modulus (soft grain with E_g=0.1E).

ships with the dimensionless indentation depth. The dimensionless indentation hardness Π_3 still shows no monotonous laws. From the result of Π_3 of both hard and soft grain cases, it is deduced that the indentation hardness is mostly a parameter of the contact surface, now that the indenter does not pierce the matrix to reach the grain, the hardness would not be affected by the impurity significantly. In contrast to this local property of the contact area, the dimensionless load and contact depth are overall properties. The hard grain increases the resistance of deformation, hence the indentation load needed increases correspondingly, due to no significant change is shown in indentation hardness, the contact area must increase to keep such increasing load, which finally reflected as the increase of the indenter contact depth. This interpretation is also verified in the case of soft grain composite, which shows opposite laws against cases of hard grain.

Combining the result from both hard and soft grain composite, Table 1 is derived to reveal the dimensionless derivative of indentation load, $\prod_7 = \frac{1}{Eh_m} \cdot \frac{\mathrm{d}F}{\mathrm{d}h}\Big|_{h=h_m}$. Π_7 changes with not only dimensionless indentation depth but also the material modulus and geometry morphology, here the most characteristic geometry $\frac{D}{d}$=0.02 is chosen and other dimensionless modulus is considered but not listed in the table. A post-processed result of that of other modulus is plotted in Figure 7, among which only $\frac{E}{Y}$=20 case is listed in Table 1. Values in Table 1 are the value of Π_7. In contrast with homogeneity, the same procedure is also applied to the homogeneous material with same dimensionless modulus and this result is listed in the first row in Table 1. It is found that Π_7 increases with dimensionless indentation depth of a hard grain composite, while an opposite law of Π_7 is shown in a soft grain composite.

For different material modulus, values of Π_7 of each indentation depth are divided by the corresponding homogenous material's value of Π_7 and plotted according to the material modulus. Π_7 is a value related to the elastic modulus of pure materials, so it is also a value describing the overall stiffness of the composite. Thus that the less the dimensionless modulus is, the smaller the stiffness is, hence the reinforcement of the hard grain would be more intensive. And for the soft grain case, Π_7 shows opposite laws which also confirms the interpretation made from hard grain case. Π_7 is a value representing the stiffness of the overall material properties and geometry of composite.

In the above analyses, all results are based on the situation that the axis of the conical indenter is collinear with the diameter of the particle. The influence of the grain beneath the indenter collinearly is very obvious, though this extreme condition is most representative, it is not the most common situation. To determine the influence of different indenter positions, several geometries are carried out with a series of the offset distance r_0, indicating the horizontal distance between the indenter axis and the centroid of the inclusion. r_0=0 indicates that the indenter axis is collinear with grain diameter. This issue is modeled by using an axisymmetric model, here the offset inclusion is actually a ring-like particle, obviously, due to the strong constraint, the influence on

Table 1 Π_7 of different grain composites and dimensionless indentation depth, with $\frac{D}{d}$=0.02 and $\frac{E}{Y}$=20

Π_7	Homogeneous	h_m/d			
		0.005	0.01	0.015	0.02
With hard grain	2.51	3.18	4.18	5.16	6.01
With soft grain	2.510	1.180	0.778	0.651	0.588

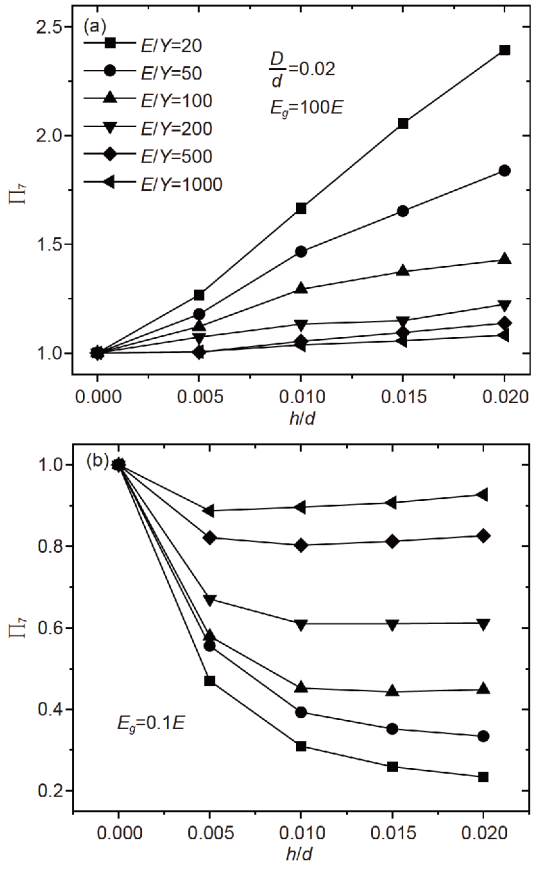

Figure 7 Ratio of Π_7 of heterogeneity to that of homogeneity. (a) Hard grain case; (b) soft grain case.

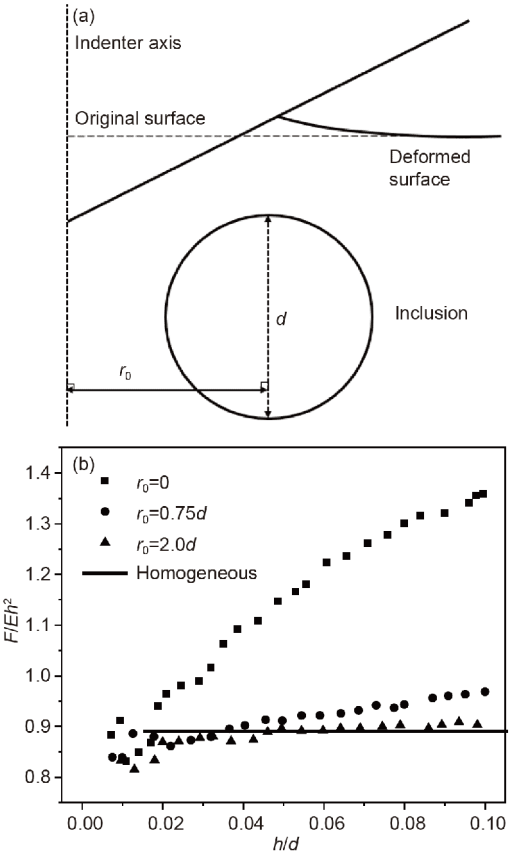

Figure 8 Geometry of indentation with offset (a) and dimensionless load with material property of E/Y=50, D/d=0.05 (b).

hardness in this case should be much larger than that the indenter axis is collinear with the spherical grain diameter.

Figure 8(a) shows the offset geometry in the axisymmetric model, and (b) shows that the dimensionless load decreases with larger offset distance rapidly, despite that the larger offset distance corresponds to the higher volume of the inclusion.

This phenomenon indicates that the discussion of the influence of inclusion on composite hardness is only significant for the case of having no offset distance or very little offset distance between indenter and the grain. This also validated the simplification of this paper that only the closest grain and conical indenter axis collinear with particle diameter are worthy of attention.

5 Summary

Through a deep conical indentation test analysis, we performed systematical research on a particle-reinforced matrix composite to investigate the scaling relationships of heterogeneous elastic-perfectly plastic material under indentation by dimensional analysis and finite element analysis based on predecessors' researches. This paper took detailed research about the influence of different particle positions and materials on the indentation response, clearly revealing the scaling relationships between heterogeneity, the indentation hardness and indentation contact area. The simplification from a complex composite to single grain composite is also validated.

Our indentation test result shows that for homogenous materials or composite with an impurity of a large distance from the surface ($\frac{D}{d} \geq 0.1$, $\frac{h}{d} \leq 0.05$), the indentation load is proportional to the square of the indenter displacement and the indentation contact depth is proportional to the indenter displacement. However, when the inclusion position is gradually approaching the indenter tip, the obtained results gradually deviate from the above relationships. The indentation response, namely, the indentation hardness, indentation contact area and load-displacement curve are sensitive with indentation parameters, e.g., the indentation depth, the stiffness of the particle, mechanical properties of the matrix, etc.

Figuring out the mechanism and basic mechanical relationships of indentation tests is of great significance in helping to reveal the indentation mechanical response and indentation size effect under small size scales.

This work was supported by the National Natural Science Foundation of China (Grant Nos. 11432014, 11672301, 11521202, 11890681).

1 Stilwell N A, Tabor D. Elastic recovery of conical indentations. Proc Phys Soc, 1961, 78: 169–179
2 Marshall D B. Mechanisms of failure from surface flaws in mixed-mode loading. J Am Ceramic Soc, 1984, 67: 110–116
3 Bhattacharya A K, Nix W D. Finite element simulation of indentation experiments. Int J Solids Struct, 1988, 24: 881–891
4 Oliver W C, Pharr G M. An improved technique for determining hardness and elastic modulus using load and displacement sensing indentation experiments. J Mater Res, 1992, 7: 1564–1583
5 Cheng Y T, Cheng C M. Can stress-strain relationships be obtained from indentation curves using conical and pyramidal indenters? J Mater Res, 1999, 14: 3493–3496
6 Cheng Y T, Cheng C M. Scaling relationships in conical indentation of elastic-perfectly plastic solids. Int J Solids Struct, 1999, 36: 1231–1243
7 Cheng Y T, Cheng C M. What is indentation hardness? Surf Coatings Tech, 2000, 133-134: 417–424
8 Shen Y L, Guo Y L. Indentation modelling of heterogeneous materials. Model Simul Mater Sci Eng, 2001, 9: 391–398
9 Shen Y L, Williams J J, Piotrowski G, et al. Correlation between tensile and indentation behavior of particle-reinforced metal matrix composites: An experimental and numerical study. Acta Mater, 2001, 49: 3219–3229
10 Ege E S, Shen Y L. Effects of inclusions and porosity on the indentation response. MRS Proc, 2002, 750: Y6.2
11 Begley M R, Hutchinson J W. The mechanics of size-dependent indentation. J Mech Phys Solids, 1998, 46: 2049–2068
12 Nix W D, Gao H. Indentation size effects in crystalline materials: A law for strain gradient plasticity. J Mech Phys Solids, 1998, 46: 411–425
13 Wei Y, Wang X, Wu X, et al. Theoretical and experimental researches of size effect in micro-indentation test. Sci China Ser A-Math, 2001, 44: 74–82
14 Wei Y, Wang X, Zhao M. Size effect measurement and characterization in nanoindentation test. J Mater Res, 2004, 19: 208–217
15 Wei Y, Shu S, Du Y, et al. Size, geometry and nonuniformity effects of surface-nanocrystalline aluminum in nanoindentation test. Int J Plast, 2005, 21: 2089–2106
16 Wei Y, Hutchinson J W. Hardness trends in micron scale indentation. J Mech Phys Solids, 2003, 51: 2037–2056
17 Chen S H, Liu L, Wang T C. Small scale, grain size and substrate effects in nano-indentation experiment of film-substrate systems. Int J Solids Struct, 2007, 44: 4492–4504
18 Huang Y, Xue Z, Gao H, et al. A study of microindentation hardness tests by mechanism-based strain gradient plasticity. J Mater Res, 2011, 15: 1786–1796
19 Zhang T Y, Xu W H, Zhao M H. The role of plastic deformation of rough surfaces in the size-dependent hardness. Acta Mater, 2004, 52: 57–68
20 Sreeram A, Patel N G, Venkatanarayanan R I, et al. Nanomechanical properties of poly(para-phenylene vinylene) determined using quasi-static and dynamic nanoindentation. Polymer Testing, 2014, 37: 86–93
21 Wang T, Zhang C, Chen S. Mechanical behaviors of carbon nanoscrolls. J Nanosci Nanotech, 2013, 13: 1136–1140
22 Sun L, Ma D, Wang L, et al. Determining indentation fracture toughness of ceramics by finite element method using virtual crack closure technique. Eng Fract Mech, 2018, 197: 151–159
23 Liu M, Tieu K A, Zhou K, et al. Indentation analysis of mechanical behaviour of torsion-processed single-crystal copper by crystal plasticity finite-element method modelling. Philos Mag, 2016, 96: 261–273
24 Bermudo C, Sevilla L, Martín F, et al. Hardening effect analysis by modular upper bound and finite element methods in indentation of aluminum, steel, titanium and superalloys. Materials, 2017, 10: 556
25 Jia H, Wu Z, Liu N. Effect of nano-ZnO with different particle size on the performance of PVDF composite membrane. Plastics Rubber Compos, 2017, 46: 1–7
26 Sivaraj M, Selvakumar N. Effect of particle size on the deformation behaviour of sintered Al-TiC nano composites. Trans Ind Inst Met, 2017, 70: 2093–2102
27 Wang C, Wang H, Xue S, et al. Size effect affected mechanical properties and formability in micro plane strain deformation process of pure nickel. J Mater Process Tech, 2018, 258: 319–325
28 Taloni A, Vodret M, Costantini G, et al. Size effects on the fracture of microscale and nanoscale materials. Nat Rev Mater, 2018, 3: 211–224
29 Krämer L, Maier-Kiener V, Champion Y, et al. Activation volume and energy of bulk metallic glasses determined by nanoindentation. Mater Des, 2018, 155: 116–124
30 Rindler A, Pöll C, Hansmann C, et al. Moisture related elastic and viscoelastic behaviour of wood adhesives by means of *in-situ* nanoindentation. Int J Adhes Adhes, 2018, 85: 123–129
31 Vgenopoulos D, Sweeney J, Grant C A, et al. Nanoindentation analysis of oriented polypropylene: Influence of elastic properties in tension and compression. Polymer, 2018, 151: 197–207
32 Kan Q, Yan W, Kang G, et al. Oliver-Pharr indentation method in determining elastic moduli of shape memory alloys—A phase transformable material. J Mech Phys Solids, 2013, 61: 2015–2033
33 Kanagaraj A B, Chaturvedi P, Alkindi T S, et al. Mechanical, thermal and electrical properties of $LiFePO_4$ /MWCNTs composite electrodes. Mater Lett, 2018, 230: 57–60
34 Lee D H, Choi I C, Yang G, et al. Activation energy for plastic flow in nanocrystalline CoCrFeMnNi high-entropy alloy: A high temperature nanoindentation study. Scripta Mater, 2018, 156: 129–133
35 O'Carroll A, Hardiman M, Tobin E F, et al. Correlation of the rain erosion performance of polymers to mechanical and surface properties measured using nanoindentation. Wear, 2018, 412-413: 38–48
36 Phadikar J K, Bogetti T A, Karlsson A M. On the uniqueness and sensitivity of indentation testing of isotropic materials. Int J Solids Struct, 2013, 50: 3242–3253